

# FLIGHT PATH RECONSTRUCTION USING THE UNSCENTED KALMAN FILTER ALGORITHM

## **Bruno Otávio Soares Teixeira**

Centro de Pesquisa e de Desenvolvimento em Engenharia Elétrica – Universidade Federal de Minas Gerais  
Laboratório de Modelagem, Análise e Controle de Sistemas Não-Lineares – MACSIN  
Av. Antônio Carlos, 6627, 31270-901, Belo Horizonte – MG, Brasil  
brunoot@cpdee.ufmg.br

## **Leonardo Antônio Borges Tôrres**

Departamento de Engenharia Eletrônica – Universidade Federal de Minas Gerais  
Laboratório de Modelagem, Análise e Controle de Sistemas Não-Lineares – MACSIN  
torres@cpdee.ufmg.br

## **Paulo Henriques Iscold Andrade de Oliveira**

Departamento de Engenharia Mecânica – Universidade Federal de Minas Gerais  
Centro de Estudos Aeronáuticos – CEA  
iscold@demec.ufmg.br

## **Luis Antonio Aguirre**

Departamento de Engenharia Eletrônica – Universidade Federal de Minas Gerais  
Laboratório de Modelagem, Análise e Controle de Sistemas Não-Lineares – MACSIN  
aguirre@cpdee.ufmg.br

**Abstract.** *This paper illustrates the application of the Flight Path Reconstruction procedure to both simulated and real data collected from a sailplane aircraft. In both cases a specific type of Sigma-Point Kalman Filter, known as the Unscented Kalman Filter (UKF), is employed to determine the biases associated to each accelerometer and gyro in the Inertial Measurement Unit (IMU), together with high sampling rate trajectory reconstruction from low frequency sampled GPS data.*

**Keywords:** *Flight Path Reconstruction, Unscented Kalman Filter, GPS and Inertial fusion*

## **1. Introduction**

Currently, there has been much effort towards the use of efficient algorithms to determine aircraft control and stability derivatives, not only from wind tunnel experiments or Computational Fluid Dynamics analysis, but also based on real data collected by onboard instrumentation, during flight tests [Jategaonkar et al., 2004, Jategaonkar and Thielecke, 2002].

The problem of Flight Path Reconstruction (FPR) is the first step in the procedure of using flight tests data to obtain information about the parameters of the aircraft model [Mulder et al., 1999]. Roughly, this reconstruction means the estimation of aircraft trajectory, based on aircraft sensors data. This step is crucial and fundamental, because real sensors do present bias and sensitivity mismatches that must be accounted for in the subsequent phases of the analysis. Estimated values for bias and sensitivity terms can be obtained in the process of flight trajectory reconstruction.

The original work on Kalman filtering [Kalman, 1960] gave rise to a very popular approach: the Extended Kalman Filter (EKF) [Haykin, 2001] that relies on linearization in order to propagate the state covariance matrix of the dynamical system. In some cases this can lead to unbounded estimation error estimates. One such instance is observed when the system is described by highly nonlinear equations as in the kinematic analysis of 6 degrees of freedom rigid bodies. Among many alternatives to the EKF, one can highlight the so-called Sigma-Point Kalman Filter (SPKF) and derivatives [van der Merwe et al., 2004] which are based on the propagation of the state covariance matrix using the ensemble statistics generated by suitably chosen points — the *sigma-points* — around the estimated state in the state space.

This paper illustrates the application of the FPR procedure to both simulated and real data collected from a sailplane aircraft. In both cases a specific type of SPKF, known as the Unscented Kalman Filter (UKF) [Julier and Uhlmann, 2004, Julier et al., 1995], is employed to determine the biases associated to each accelerometer and gyro in the IMU, together with high sampling rate trajectory reconstruction from low frequency sampled GPS<sup>1</sup> data.

The paper is organized as follows. In Section 2, the problem of state vector recursive estimation is presented in this general form. In Section 3, the UKF algorithm is presented, together with a smoothing algorithm employed to enhance the state estimation by means of offline computations. The problem of FPR is cast in terms of nonlinear recursive state

---

<sup>1</sup>Global Positioning System.

vector estimation in Section 3.2. Simulation results are presented in Section 3.3. In Section 4, the algorithm is used in a real case. The data was obtained from flight tests on a sailplane aircraft. Finally, the main paper conclusions are presented in Section 5.

## 2. Problem Description

The state estimation problem for the continuous-time nonlinear dynamical system

$$\begin{cases} \dot{\mathbf{x}}_t = f[\mathbf{x}_t, \mathbf{u}_t, \mathbf{w}_t], \\ \mathbf{y}_t = h[\mathbf{x}_t, \mathbf{r}_t], \end{cases} \quad (1)$$

where  $f[\cdot]$  and  $h[\cdot]$  are respectively the assumed known process and observation models, can be described as follows. Suppose that the only known data are the initial conditions  $\mathbf{x}(0) \in \mathbb{R}^n$ , the measurements  $\mathbf{y}_t \in \mathbb{R}^m$  and the control inputs  $\mathbf{u}_t \in \mathbb{R}^p$ ,  $\forall t > 0$ . Process noise  $\mathbf{w}_t \in \mathbb{R}^n$  and measurement noise  $\mathbf{r}_t \in \mathbb{R}^m$  are assumed white, Gaussian, zero-mean and mutually independent with covariance matrices  $Q$  and  $R$ , respectively. It is desired to obtain an estimate for the unobserved state vector  $\mathbf{x}_t$ ,  $\forall t > 0$ .

## 3. The UKF Algorithm

Many difficulties associated to the EKF have been partially circumvented by the use of the UKF which is based on the intuition that it should be easier to approximate a Gaussian distribution than an arbitrary nonlinear function [Julier et al., 1995]. Instead of linearizing the model equations, this algorithm propagates a small representative group of deterministically chosen points (actually vectors) named sigma points:  $\mathcal{X}_i$ ,  $i = 0, 1, \dots, 2n_a$ , where  $n_a$  is the dimension of the augmented state vector — which by construction includes the mean and covariance information of the state estimate at time  $k - 1$ , with  $t = kT_s$  where  $k$  denotes discrete time and  $T_s$  is the sampling period, in order to numerically calculate the prior state estimate  $\hat{\mathbf{x}}_{k|k-1}$  and its covariance matrix  $P_{k|k-1}$  by their propagation through the discrete counterpart of the nonlinear equations (1). Hence, the algorithm can be implemented as follows.

Firstly, an augmented state vector is composed by the concatenation of the original state, process and measurement noise variables thus  $\mathbf{x}_k^a = [\mathbf{x}_k^T \ \mathbf{w}_k^T \ \mathbf{r}_k^T]^T$ , and  $\mathbf{x}_k^a \in \mathbb{R}^{n_a}$  where  $n_a = 2n + m$ . Consequently the covariance matrix of the vector of estimation errors must refer to this augmented state vector and henceforth it will be referred to as  $P^a \in \mathbb{R}^{(2n+m) \times (2n+m)}$ , that is

$$P^a = \begin{bmatrix} P & 0 & 0 \\ 0 & Q & 0 \\ 0 & 0 & R \end{bmatrix}. \quad (2)$$

The sigma points can be chosen as

$$\begin{cases} \mathcal{X}_{0, k-1|k-1}^a = \hat{\mathbf{x}}_{k-1|k-1}^a \\ \mathcal{X}_{i, k-1|k-1}^a = \hat{\mathbf{x}}_{k-1|k-1}^a + \left[ \sqrt{(n_a + \lambda) P_{k-1|k-1}^a} \right]_i \\ \mathcal{X}_{i+n_a, k-1|k-1}^a = \hat{\mathbf{x}}_{k-1|k-1}^a - \left[ \sqrt{(n_a + \lambda) P_{k-1|k-1}^a} \right]_i, \end{cases} \quad (3)$$

with associated weights given by

$$\begin{cases} w_0^{(m)} = \frac{\lambda}{n_a + \lambda} \\ w_0^{(c)} = \frac{\lambda}{n_a + \lambda} + 1 - \alpha^2 + \beta \\ w_i^{(m)} = w_i^{(c)} = \frac{1}{2(n_a + \lambda)}, \end{cases} \quad (4)$$

with  $i = 1, \dots, n_a$  and  $[\sqrt{\cdot}]_i$  is either the  $i$  th row or column of the matrix square-root [Julier and Uhlmann, 2004]. For the sake of simplicity the following choices are made  $\lambda = \alpha^2(\kappa + n_a) - n_a = 0$  [Julier and Uhlmann, 2004]  $\alpha = 1$ ,  $\kappa = 0$  and  $\beta = 2$  [Haykin, 2001]. Choosing the sigma points as indicated in (3) guarantees exact matching of the first three moments. The unscented Kalman filter equations can be expressed as [Julier and Uhlmann, 2004, Haykin, 2001]

$$\begin{cases} \hat{\mathbf{x}}_{k|k-1} = \sum_{i=0}^{2n_a} w_i^{(m)} \mathcal{X}_{i, k|k-1}^x, \quad \text{where } \mathcal{X}_{i, k|k-1}^x = f[\mathcal{X}_{i, k-1|k-1}^x, \mathbf{u}_{k-1}, \mathcal{X}_{i, k-1|k-1}^w] \\ \hat{\mathbf{y}}_{k|k-1} = \sum_{i=0}^{2n_a} w_i^{(m)} \mathcal{Y}_{i, k|k-1}, \quad \text{where } \mathcal{Y}_{i, k|k-1} = h[\mathcal{X}_{i, k|k-1}^x, \mathcal{X}_{i, k|k-1}^r] \\ P_{k|k-1} = \sum_{i=0}^{2n_a} w_i^{(c)} [\mathcal{X}_{i, k|k-1}^x - \hat{\mathbf{x}}_{i, k|k-1}] [\mathcal{X}_{i, k|k-1}^x - \hat{\mathbf{x}}_{i, k|k-1}]^T \\ P_{k|k-1}^{yy} = \sum_{i=0}^{2n_a} w_i^{(c)} [\mathcal{Y}_{i, k|k-1} - \hat{\mathbf{y}}_{i, k|k-1}] [\mathcal{Y}_{i, k|k-1} - \hat{\mathbf{y}}_{i, k|k-1}]^T \\ P_{k|k-1}^{xy} = \sum_{i=0}^{2n_a} w_i^{(c)} [\mathcal{X}_{i, k|k-1}^x - \hat{\mathbf{x}}_{i, k|k-1}] [\mathcal{Y}_{i, k|k-1} - \hat{\mathbf{y}}_{i, k|k-1}]^T \\ K_k = P_{k|k-1}^{xy} \left[ P_{k|k-1}^{yy} \right]^{-1}, \end{cases} \quad (5)$$

with  $i = 0, \dots, 2n_a$  and where  $\mathcal{X}_{i, k-1|k-1}^a$  are given by (3) and  $\mathcal{X}^a = [(\mathcal{X}^x)^T (\mathcal{X}^w)^T (\mathcal{X}^r)^T]^T$ . The set of equations (5) forms the *prediction or propagation* step of the UKF that propagates the state estimate one step ahead using the process model. In the case of a continuous-time dynamical system, the state estimate at  $t = (k-1)T_s$  (represented by the sigma points  $\mathcal{X}_{k-1|k-1}^a$ ) can be used as initial conditions to numerically integrate equations (1) one step ahead. This way the discrete form of the UKF algorithm can be readily used.

The *updating or correction* equations are

$$\begin{cases} \hat{\mathbf{x}}_{k|k} = \hat{\mathbf{x}}_{k|k-1} + K_k [\mathbf{y}_k - h[\hat{\mathbf{x}}_{k|k-1}]] \\ P_{k|k} = P_{k|k-1} - K_k P_{k|k-1}^y K_k^T \end{cases} \quad (6)$$

For details on Kalman filtering in general, the reader is referred to [Maybeck, 1979, Crassidis and Junkis, 2004] and for the UKF see [Julier and Uhlmann, 2004, Haykin, 2001] and references therein.

### 3.1 The UKS Algorithm

In the previous section the UKF was presented as a recursive algorithm that provides estimates of the state vector  $\hat{\mathbf{x}}_{k|k}$  based on all past and present measurement vectors  $\mathbf{y}_1, \mathbf{y}_2, \dots, \mathbf{y}_k$ . In the case of offline estimation, such as the FPR problem, the Unscented Kalman Smoother (UKS) [Haykin, 2001] may be employed to produce improved estimates (the measurement noise effects are smoothed out further) by the use of future measurements  $\mathbf{y}_{k+1}, \mathbf{y}_{k+2}, \dots, \mathbf{y}_N$ , where  $N$  equals the total length of the flight test data. To achieve this goal, the UKS optimally combines the results of a forward and a backward UKF. The former estimates mean and covariance ( $\hat{\mathbf{x}}_{k|k}^f, P_{k|k}^f$ ) given past and present data, and the latter estimates ( $\hat{\mathbf{x}}_{k|k+1}^b, P_{k|k+1}^b$ ) given future data. The forward UKF is implemented exactly as shown by equations (5) and (6) whereas the backward UKF can make use of the following backward counterpart continuous-time model before applying the same algorithm:

$$\begin{cases} \dot{\mathbf{x}}_{-t} = -f[\mathbf{x}_{-t}, \mathbf{u}_{-t}, \mathbf{w}_{-t}] \\ \mathbf{y}_{-t} = h[\mathbf{x}_{-t}, \mathbf{r}_{-t}], \end{cases} \quad (7)$$

where  $-t$  denotes time inversion of input and output data. The optimal way that the UKS combines the forward and backward filter results in order to produce the smoothed mean and covariance ( $\hat{\mathbf{x}}_k^s, P_k^s$ ) of the states is given by the following equations

$$\begin{cases} [P_k^s]^{-1} = [P_{k|k}^f]^{-1} + [P_{k|k+1}^b]^{-1} \\ \hat{\mathbf{x}}_k^s = P_k^s \left[ [P_{k|k}^f]^{-1} \hat{\mathbf{x}}_{k|k}^f + [P_{k|k+1}^b]^{-1} \hat{\mathbf{x}}_{k|k+1}^b \right]. \end{cases} \quad (8)$$

When it comes to online applications, the iterative Kalman filter may reduce the effect of observation equation nonlinearities (recall that the UKF is a kind of a second-order EKF in terms of accuracy), improving the current state estimate by applying local iterations to repeatedly calculate  $\mathbf{x}_{k|k}, P_{k|k}$  and  $K_k$ .<sup>2</sup> In the case of EKF, the iterative approach requires the local linearization of the observation model in each iteration [Crassidis and Junkis, 2004]. Similarly, in the context of the UKF, new sigma points (3) should be calculated at each iteration, an issue that will be treated in a future paper.

Besides reducing the effect of observation nonlinearities, given that slowly sampled observations — such as the ones provided by some GPS receivers — can be used, the aforementioned approaches somewhat play the role of interpolators, which helps to mitigate the abrupt artificial changes in the position variables that appear in the estimates.

### 3.2 FPR and the UKF algorithm

In the FPR problem, kinematic models are used to describe the temporal evolution of a six degrees of freedom rigid body. These equations consists of three sets of nonlinear first-order ordinary differential equations (ODE) as follows. The first set describe how the translational velocity components  $u, v$  and  $w$ , along the rigid body axes, evolves with time:

$$\begin{cases} \dot{u} = -q w + r v - g \sin \theta + A_x, \\ \dot{v} = -r u + p w + g \cos \theta \sin \phi + A_y, \\ \dot{w} = -p v + q u + g \cos \theta \cos \phi + A_z. \end{cases} \quad (9)$$

The second set accounts for the rotational dynamics through the time histories of the Euler angles  $\phi, \theta$  and  $\psi$  with respect to the earth-fixed reference frame:

$$\begin{cases} \dot{\phi} = -p + q \sin \phi \tan \theta + r \cos \phi \tan \theta, \\ \dot{\theta} = q \cos \phi - r \sin \phi, \\ \dot{\psi} = q \sin \phi \sec \theta + r \cos \phi \sec \theta. \end{cases} \quad (10)$$

Finally, numerically integrating the following set of ODE together with Equations (9) and (10) the position of the aircraft's c.g. ( $x_E, y_E, H$ ) relative to the earth-fixed reference may be determined:

<sup>2</sup>According to [Mulder et al., 1999] four to eight iterations are generally employed in FPR.

$$\begin{bmatrix} \dot{x}_E \\ \dot{y}_E \\ \dot{H} \end{bmatrix} = L_{EB} \begin{bmatrix} u \\ v \\ w \end{bmatrix} + \begin{bmatrix} W_{x_E} \\ W_{y_E} \\ W_H \end{bmatrix}, \quad (11)$$

where the orthogonal matrix  $L_{EB}$  relates the fixed-earth and rigid body reference frames

$$L_{EB} = \begin{bmatrix} \cos \theta \cos \psi & \sin \phi \sin \theta \cos \psi - \cos \phi \sin \psi & \cos \phi \sin \theta \cos \psi + \sin \phi \sin \psi \\ \cos \theta \sin \psi & \sin \phi \sin \theta \sin \psi + \cos \phi \cos \psi & \cos \phi \sin \theta \sin \psi - \sin \phi \cos \psi \\ -\sin \theta & \sin \phi \cos \theta & \cos \phi \cos \theta \end{bmatrix}, \quad (12)$$

and  $W_{x_E}$ ,  $W_{y_E}$  and  $W_H$  account for the components of a generally assumed constant atmospheric wind vector along the earth-fixed reference frame. At this point, it is important to emphasize that Equations (9), (10) and (11) form the nonlinear kinematic *process* model of an airplane (or any rigid body) in state space, where the states  $\mathbf{x}_t \in \mathbb{R}^9$  are given by

$$\mathbf{x}_t = [u \ v \ w \ \phi \ \theta \ \psi \ x_E \ y_E \ H]^T, \quad (13)$$

and the aerodynamic forces and the angular rates play the role of inputs  $\mathbf{u}_k \in \mathbb{R}^6$  as

$$\mathbf{u}_k = [A_{x,m} \ A_{y,m} \ A_{z,m} \ p_m \ q_m \ r_m]^T. \quad (14)$$

where the subscript  $m$  identifies that the variable is measured by onboard instrumentation. The state space dynamical model is completed by considering the *observation* equations whose measurement vector  $\mathbf{y}_k \in \mathbb{R}^9$  can be compound by the following variables

$$\mathbf{y}_k = [\phi_m \ \theta_m \ \psi_m \ V_{TAS,m} \ \alpha_m \ \beta_m \ x_{E,m} \ y_{E,m} \ H_m]^T, \quad (15)$$

with the Euler angles  $\phi_m$ ,  $\theta_m$  and  $\psi_m$  also generally given by the IMU,  $V_{TAS,m}$  is the true airspeed measured directly by means of an anemometer or a Pitot tube system,  $\alpha_m$  and  $\beta_m$  are respectively the attack and sideslip angles measured by vanes,  $x_{E,m}$  and  $y_{E,m}$  are the geographical coordinates provided by GPS receivers and  $H$  refers to the altitude (or the  $z_E$  position coordinate in the fixed-earth frame) given by barometric sensors.

Thus the complete state space dynamical model of an aircraft used in FPR can be given by

$$\dot{\mathbf{x}}_t = f[\mathbf{x}_t, \mathbf{u}_{kT_s}, \mathbf{w}_{kT_s}] = \begin{bmatrix} -(q_m - \Delta_q)w + (r_m - \Delta_r)v - g \sin \theta + (A_{x,m} - \Delta_{A_x}) \\ -(r_m - \Delta_r)u + (p_m - \Delta_p)w + g \cos \theta \sin \phi + (A_{y,m} - \Delta_{A_y}) \\ -(p_m - \Delta_p)v + (q_m - \Delta_q)u + g \cos \theta \cos \phi + (A_{z,m} - \Delta_{A_z}) \\ (p_m - \Delta_p) + (q_m - \Delta_q) \sin \phi \tan \theta + (r_m - \Delta_r) \cos \phi \tan \theta \\ (q_m - \Delta_q) \cos \phi - (r_m - \Delta_r) \sin \phi \\ (q_m - \Delta_q) \sin \phi \sec \theta + (r_m - \Delta_r) \cos \phi \sec \theta \\ [L_{EB}]_1 u + W_{x_E} \\ [L_{EB}]_2 v + W_{y_E} \\ [L_{EB}]_3 w + W_H \end{bmatrix} + \begin{bmatrix} w_u \\ w_v \\ w_w \\ w_\phi \\ w_\theta \\ w_\psi \\ w_{x_E} \\ w_{y_E} \\ w_H \end{bmatrix}, \quad (16)$$

$$\mathbf{y}_k = h[\mathbf{x}_{\frac{t}{T_s}}, \mathbf{r}_k] = \begin{bmatrix} K_\phi \phi + \Delta_\phi \\ K_\theta \theta + \Delta_\theta \\ K_\psi \psi + \Delta_\psi \\ K_V \sqrt{u^2 + v^2 + w^2} + \Delta_{V_T} \\ K_\alpha \arctan\left(\frac{w}{u}\right) + \Delta_\alpha \\ K_\beta \arctan\left(\frac{v}{\sqrt{u^2 + w^2}}\right) + \Delta_\beta \\ K_{x_E} x_E + \Delta_{x_E} \\ K_{y_E} y_E + \Delta_{y_E} \\ K_H H + \Delta_H \end{bmatrix} + \begin{bmatrix} r_{\phi_m} \\ r_{\theta_m} \\ r_{\psi_m} \\ r_{V_{TAS,m}} \\ r_{\alpha_m} \\ r_{\beta_m} \\ r_{x_{E,m}} \\ r_{y_{E,m}} \\ r_{H_m} \end{bmatrix}, \quad (17)$$

where the *measured* inputs  $\mathbf{u}_k$  (14) discounts the respective bias (indicated as  $\Delta_u$ ,  $u$  refers to all components of  $\mathbf{u}_k$ ) in equations (16) whereas all outputs  $\mathbf{y}_k$  (15) regards about it ( $\Delta_y$ ,  $y$  refers to all components of  $\mathbf{y}_k$ ) in (17) besides related scale factors (given by  $K_y$ ,  $y$  substitutes all elements of the vector  $\mathbf{y}_k$ ) and both process and measurement noise vectors,  $\mathbf{w}_k$  and  $\mathbf{r}_k$ , are assumed additive.

And last but not least, since the UKF algorithm can be also readily used to jointly estimate system parameters, it is easy to consider a parameter as a “virtual” state. Thus equations (16) can be extended so as to take into account the bias and scale factor effects. In this paper only bias variables are jointly estimated. Although, at first sight, this approach seems simplistic it was successfully employed in [Mulder et al., 1999, van der Merwe et al., 2004]. Moreover too many parameters may lead to nonreconstructible components in the extended state vector. Therefore vector (13) can be concatenated with  $\theta_t \in \mathbb{R}^{p_\theta}$

$$\theta_t = [\Delta_{A_x} \ \Delta_{A_y} \ \Delta_{A_z} \ \Delta_p \ \Delta_q \ \Delta_r \ \Delta_\phi \ \Delta_\theta \ \Delta_\psi \ \Delta_{V_T} \ \Delta_\alpha \ \Delta_\beta \ \Delta_{x_E} \ \Delta_{y_E} \ \Delta_H]^T, \quad (18)$$

so that  $\mathbf{x}_{e,x,t,t} = [\mathbf{x}_t^T \ \theta_t^T]^T$  and equations (16) can be extended by

$$\dot{\theta}_t = -\frac{1}{\tau}\theta_t + \mathbf{w}_{\theta,t}, \quad (19)$$

where  $\tau$  is the correlation time that governs the temporal evolution of the parameters  $\theta$  according to a zero-mean stationary first-order Markov process [Mulder et al., 1999]. Taking  $\tau$  to infinity, the parameter dynamics is modelled as a random walk stochastic process that is able to deal with non-zero mean and non-stationary behaviour of some IMU sensors for instance [van der Merwe et al., 2004].

Often it is expected that the system parameters do not vary or, if they do, the variation is much slower than that of the original system state. Then, in both cases, the parameter covariance matrix  $Q_\theta \in \mathbb{R}^{n_\theta \times n_\theta}$  of the Gaussian, zero-mean and white-noise random variables  $\mathbf{w}_\theta$  accounts for the uncertainty in the estimated parameters and permit their variation with time.<sup>3</sup> Lower-bounding the parameter error covariance matrix  $P_\theta$  by suitably setting a non-null  $Q_\theta$  allows to emphasize the most recent data  $\mathbf{y}_k$  preventing the algorithm from stalling.

### 3.3 Simulation Results

This section reports some tests conducted with simulated data obtained by the FDC toolbox [Rauw, 2005]. This Simulink toolbox models a DHC-2 Beaver aircraft by coupling aerodynamic, atmospheric, gravity and propulsion engine equations in a flat-earth nonlinear state space dynamic model. The states, inputs and outputs are given by equations (13), (14) and (15) respectively.

The FPR problem discussed in Section 3.2 is treated here by investigating two types of trajectories. Both very rapid and smoother maneuvers are shown in Fig. 1. It is important to note that the very rapid maneuver shown in Figure 1.a is likely to be unfeasible for the appointed simulation time span of 60s, due to aircraft physical constraints. However, this data set was important to reveal best practices in conducting flight tests, particularly related to sensors parameters estimation.

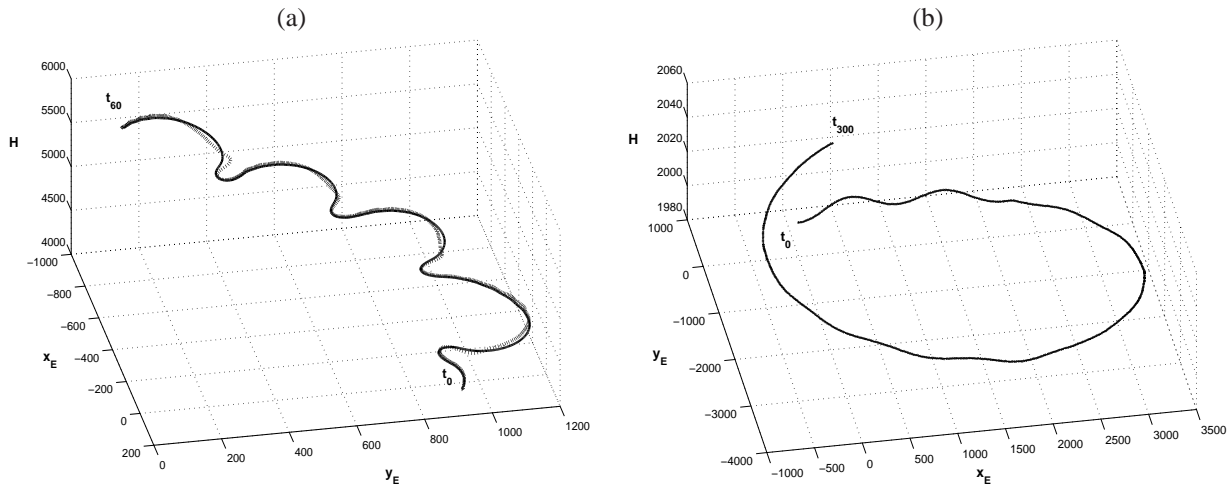


Figure 1. Simulated (—) and reconstructed ( . . . ) Beaver trajectories: (a) the very rapid one was obtained integrating model equations at  $\delta t = 0.005s$  during 60s whereas (b) for the smoother it was used  $\delta t = 0.01s$  during 300s. In both cases the reconstruction considered  $T_s = 0.10s$  for all inputs and outputs, except for the GPS measurements ( $T_{GPS} = 1.0s$ ).

Indeed, as can be inferred from the values in Tables 1 and 2, if the initial goal is to estimate bias from the IMU sensors, one should employ data sets corresponding to smooth maneuvers. This seems to be consistent with the fact that steady state flight conditions are more adequate to reveal the effect of accelerometers and gyro biases, because in those cases these mismatches rapidly lead to large errors that can be detected easier than those observed in very rapid and oscillating maneuvers.

Despite this, the state estimation errors for the smooth maneuver case reveal that the algorithm is relatively robust to noise in the IMU sensors. The state estimation errors are small, as shown in Table 1 (below 10% even in the worst case) for noise levels ranging from 1% to 25% in the signals provided by the IMU and by the outputs (15).

<sup>3</sup>The greater is the trace of  $Q_\theta$ , the quicker are the permitted variations in  $\theta$ . Different approaches, namely, fixed or time-varying  $Q_\theta$ , can be used to tune UKF convergence rate and parameters tracking performance [Haykin, 2001]. For the sake of simplicity, in the present work  $Q_\theta$  will be taken as a constant matrix.

Table 1. Root mean square (RMS) and normalized RMS (in italic) errors of estimated states for Beaver simulated data (both smooth and rapid trajectories) regarding different signal-to-noise ratios (SNR) in inputs and outputs.

Traj./SNR	$u$ (m/s) (%)	$v$ (m/s) (%)	$w$ (m/s) (%)	$\phi$ (rad) (%)	$\theta$ (rad) (%)	$\psi$ (rad) (%)	$x_E$ (m) (%)	$y_E$ (m) (%)	$H$ (m) (%)
Smooth 1%	0.0015	0.0027	0.0004	0.0001	0.0001	0.1404	3.4426	3.8446	0.1405
	<i>0.0034</i>	<i>0.0711</i>	<i>0.0059</i>	<i>0.0810</i>	<i>0.0258</i>	<i>4.4705</i>	<i>0.1081</i>	<i>0.0844</i>	<i>0.0068</i>
Rapid 1%	1.7514	1.2325	3.0175	0.0096	0.0016	1.4469	12.6520	20.3046	24.8081
	<i>0.9407</i>	<i>2.2962</i>	<i>2.5933</i>	<i>0.5378</i>	<i>0.2293</i>	<i>46.1579</i>	<i>1.3721</i>	<i>2.0470</i>	<i>0.4264</i>
Smooth 10%	0.0088	0.0164	0.0034	0.0008	0.0003	0.2811	12.6279	13.1645	0.6067
	<i>0.0201</i>	<i>0.4364</i>	<i>0.0499</i>	<i>0.4826</i>	<i>0.1949</i>	<i>8.9474</i>	<i>0.3966</i>	<i>0.2890</i>	<i>0.0295</i>
Rapid 10%	3.3807	2.5387	4.7160	0.0159	0.0152	1.3823	50.6492	67.0234	184.6727
	<i>1.8159</i>	<i>4.7297</i>	<i>4.0530</i>	<i>0.8902</i>	<i>2.1603</i>	<i>44.0972</i>	<i>5.4928</i>	<i>6.7568</i>	<i>3.1743</i>
Smooth 25%	0.0183	0.0380	0.0082	0.0019	0.0008	0.2017	16.0906	17.6577	0.9390
	<i>0.0418</i>	<i>1.0080</i>	<i>0.1195</i>	<i>1.1033</i>	<i>0.4581</i>	<i>6.4217</i>	<i>0.5053</i>	<i>0.3877</i>	<i>0.0456</i>
Rapid 25%	11.3401	2.5624	10.4396	0.0334	0.0396	1.4381	37.6388	49.0660	207.5675
	<i>6.0910</i>	<i>4.7739</i>	<i>8.9721</i>	<i>1.8631</i>	<i>5.6101</i>	<i>45.8782</i>	<i>4.0818</i>	<i>4.9465</i>	<i>3.5679</i>

Table 2. Normalized steady-state errors of estimated IMU bias for Beaver simulated data (smooth case only) regarding different noise levels in model inputs and outputs. The following choices were made for bias values:  $\Delta_{a_x} = 0.01g$ ,  $\Delta_{a_y} = -0.05g$ ,  $\Delta_{a_z} = -0.02g$ ,  $\Delta_p = 0.5^\circ/s$ ,  $\Delta_q = -0.5^\circ/s$  and  $\Delta_r = 0.5^\circ/s$ .

SNR	$\Delta_{a_x}$ (%)	$\Delta_{a_y}$ (%)	$\Delta_{a_z}$ (%)	$\Delta_p$ (%)	$\Delta_q$ (%)	$\Delta_r$ (%)
1%	1.0896	-0.1798	3.1236	-0.0016	0.0129	0.1030
10%	1.1864	2.7973	3.9169	0.2442	-0.1767	-3.4034
25%	0.9622	-3.8705	2.0931	-0.7857	0.0858	4.6997

For the rapid maneuver, the state estimation error worst case was observed for  $\psi$ . This seems to be due to the artificial discontinuity introduced when the yaw angle traverses the  $2\pi$  boundary. This is another strong indication that one should employ quaternions [Stevens and Lewis, 1992], instead of Euler angles, to estimate rigid body attitude.

The results obtained for sensors biases estimation are shown in Table 2. No convergence was obtained for the rapid maneuver case. Two different approaches were used to model the parameters dynamics, as indicated in Equation (19): Markovian ( $0 < \tau < \infty$ ) and random-walk ( $\tau \rightarrow \infty$ ) strategies. Only results for the latter approach are presented, although it is important to remark that similar results were observed in both cases.

#### 4. Experimental Data – Sailplane Aircraft

In order to verify the efficiency of the UKF algorithm in a real case, the procedure described in Section 3. was employed to estimate states and parameters from data collected in flight tests conducted on a SZD 50-3 Puchacz sailplane [PZL-Bielsko, 2005] (see Figure 2), piloted by one of the authors. This aircraft is manufactured in fiberglass, with 16.67m wingspan and empty weight between 360Kg and 370Kg. The flight tests data were kindly provided by the Centro de Estudos Aeronáuticos – CEA/UFMG [Centro de Estudos Aeronáuticos – CEA, 2005].

The Flight Data Acquisition System – FDAS; i.e. the onboard instrumentation; was developed in the CEA/UFMG and comprises an airdata probe capable of measuring static and dynamic pressures, and angles of attack and sideslip; and accompanying sensors to measure outside air temperature, flight controls positions, and aircraft accelerations using MEMS<sup>4</sup> accelerometers. The angular velocities and translational accelerations were provided by a MicroStrain 3DM-GX1 IMU, which was connected to a portable computer. The inertial data collected using the commercial IMU was properly synchronized with the rest of the acquired data collected using the FDAS-CEA system by means of the MEMS accelerometers signals.

The maneuvers were planned to properly excite the aircraft longitudinal (phugoid and short period) and lateral-directional modes. Time series for the estimated attitude and translational velocities are shown in Figure 3.

In Table 3 real results obtained from the Puchacz sailplane aircraft flight tests data are presented. The percentual errors in the translational velocities were obtained considering that the variables  $V_T$ ,  $\alpha$  and  $\beta$  were perfectly measured, i.e. the airdata probe was considered our calibration standard. In the same way, the attitude information, that was provided by the commercial IMU, and the low frequency GPS data were assumed to be perfect measurements.

The results reveal that the UKS procedure can be effectively used to improve the estimation of high frequency sampled data from low frequency sampled acquired data (GPS measurements), which seems to be consistent with the discussion in Section 3.1.

<sup>4</sup>Microelectromechanical devices.

Based on the apparently small values observed for the state estimation errors, it seems that the results obtained for sensor biases estimation, shown in Figure 4, could be regarded as good approximations of the real sensors parameters. However, it is important to emphasize that it was not possible to validate this conclusion once there was no independent account for the sensor biases.

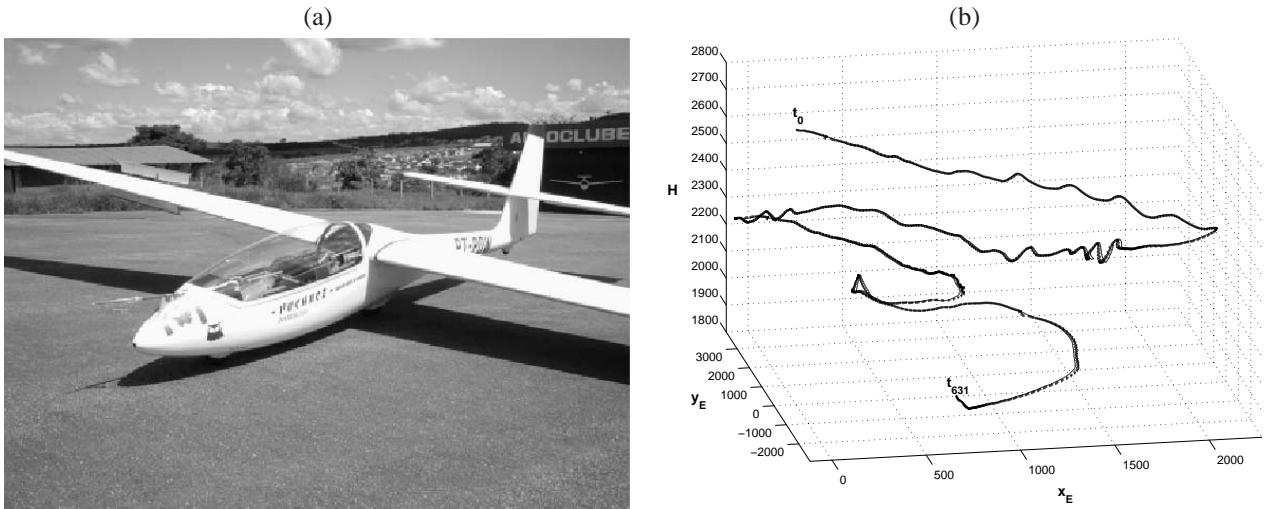


Figure 2. (a) SZD 50-3 Puchacz sailplane. (b) Real (—) and reconstructed (···) aircraft trajectories. The flight path reconstruction considered  $T_s = 0.10s$  for all inputs and outputs, except for the GPS measurements ( $T_{GPS} = 1.0s$ ).

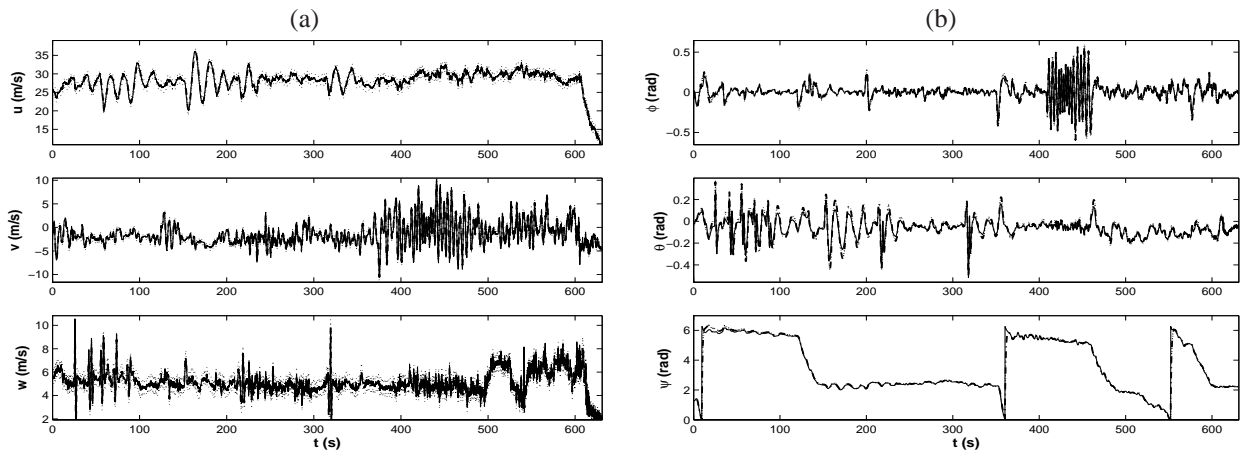


Figure 3. Real (—) and UKF joint estimated (---) velocity components ( $u$ ,  $v$  e  $w$ ) and Euler angles ( $\phi$ ,  $\theta$  e  $\psi$ ) of SZD 50-3 Puchacz sailplanes's trajectory shown in Fig. 2. It is important to note the discontinuity on  $\psi$ .

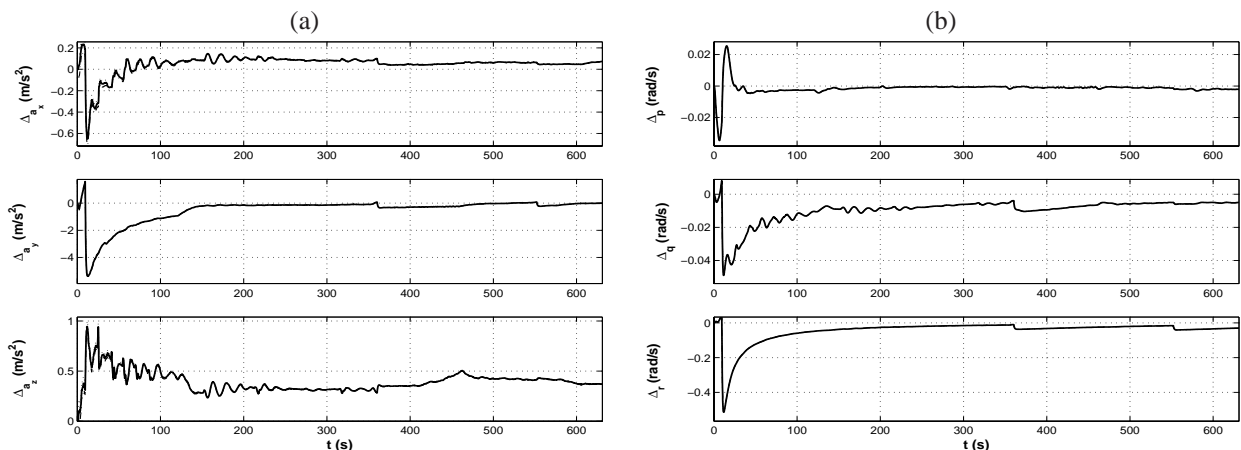


Figure 4. UKF joint estimated (—) IMU sensor biases of SZD 50-3 Puchacz sailplane.

Table 3. Root mean square (RMS) and normalized RMS (in italic) errors of estimated states for Puchacz data for UKF and UKS algorithms.

Traj./SNR	$u$ (m/s) (%)	$v$ (m/s) (%)	$w$ (m/s) (%)	$\phi$ (rad) (%)	$\theta$ (rad) (%)	$\psi$ (rad) (%)	$x_E$ (m) (%)	$y_E$ (m) (%)	$H$ (m) (%)
UKF	0.3685	0.2758	0.1897	0.0224	0.0274	0.2622	10.5580	11.8034	1.0979
	<i>1.0203</i>	<i>2.6481</i>	<i>1.7978</i>	<i>4.4328</i>	<i>5.3115</i>	<i>4.1836</i>	<i>0.5126</i>	<i>0.3389</i>	<i>0.0389</i>
UKS	0.2136	0.1412	0.1079	0.0149	0.0111	0.0964	2.5140	3.3916	0.4935
	<i>0.5914</i>	<i>1.3548</i>	<i>1.0228</i>	<i>2.9335</i>	<i>2.1569</i>	<i>3.0689</i>	<i>0.1220</i>	<i>0.0973</i>	<i>0.0174</i>

## 5. Concluding Remarks

In this paper a Kalman Filter like algorithm – known as the Unscented Kalman Filter – UKF was presented as a viable alternative to perform Flight Path Reconstruction without relying on kinematic equations linearization.

Together with the aforementioned algorithm, a derivated smoothing procedure was also presented. This procedure leads to the Unscented Kalman Smoother (Section 3.1), which can be used to enhance the quality of the estimation by combining future and past data in offline calculations to generate smoother high frequency sampled trajectory reconstruction from low frequency GPS data.

As discussed in Section 3.3, the flight tests should be conducted so that slowing varying or even static measurements from the onboard sensors are obtained, in order to facilitate the estimation of sensors biases.

The UKF algorithm convergence is greatly affected by the initial process and measurement noise covariance matrices. The initial covariance estimate can be obtained from instrumentation technical specifications related to overall accuracy and precision. It is important to note that there exist the possibility of estimating the noise statistics altogether, which is called adaptive filtering. A deeper analysis in this case is under way.

## 6. Acknowledgements

The authors are grateful to CAPES and CNPq for financial support.

## 7. References

- Centro de Estudos Aeronáuticos – CEA (2005). Internet site. <http://www.demec.ufmg.br/cea>.
- Crassidis, J. L. and Junkis, J. L. (2004). *Optimal Estimation of Dynamic Systems*. Chapman & Hall/CRC, Boca Raton.
- Haykin, S. (2001). *Kalman Filtering and Neural Networks*. Wiley Publishing, New York.
- Jategaonkar, R., Fischenberg, D., and von Gruenhagen, W. (2004). Aerodynamic modeling and system identification from flight data - recent applications at DLR. *Journal of Aircraft*, 41(4):681–691.
- Jategaonkar, R. and Thielecke, F. (2002). ESTIMA – an integrated software tool for nonlinear parameter estimation. *Aerospace Science and Technology*, 6(8):565–578.
- Julier, S. J. and Uhlmann, J. K. (2004). Unscented filtering and nonlinear estimation. *Proceedings of the IEEE*, 92(3):401–422.
- Julier, S. J., Uhlmann, J. K., and Durrant-Whyte, H. F. (1995). A new approach for filtering nonlinear systems. In *The Proceedings of the American Control Conference*, pages 1628–1632, Seattle, Washington.
- Kalman, R. E. (1960). A new approach to linear filtering and prediction problems. *Transactions of the ASME-Journal of Basic Engineering*, 82:35–45.
- Maybeck, P. S. (1979). *Stochastic Models, Estimation and Control*, volume 1. Academic Press, San Diego.
- Mulder, J. A., Chu, Q. P., Sridhar, J. K., Breeman, J., and Laban, M. (1999). Non-linear aircraft flight path reconstruction review and new advances. *Progress in Aerospace Sciences*, 35:673–726.
- PZL-Bielsko (2005). SZD 50-3 Puchacz – Internet site. <http://www.szdusa.com/50.html>.
- Rauw, M. O. (2005). FDC 1.4 - A Simulink Toolbox for Flight Dynamics and Control Analysis. Technical report, <http://home.wanadoo.nl/dutchroll/index.html>.
- Stevens, B. L. and Lewis, F. L. (1992). *Aircraft Control and Simulation*. John Wiley & sons, Inc.
- van der Merwe, R., Wan, E., and Julier, S. (2004). Sigma-point kalman filters for nonlinear estimation and sensor-fusion: Applications to integrated navigation. In *AIAA Guidance, Navigation and Control Conference and Exhibit*, Providence, Rhode Island. AIAA – American Institute of Aeronautics and Astronautics.